Available online at www.eccomasproceedia.org
Eccomas Proceedia COMPDYN (2019) 4376-4385

ECCOMAS
Proceedia

COMPDYN 2019
7th ECCOMAS Thematic Conference on
Computational Methods in Structural Dynamics and Earthquake Engineering
M. Papadrakakis, M. Fragiadakis (eds.)
Crete, Greece, 24–26 June 2019

DYNAMIC MAGNIFICATION FACTORS FOR SNOW AVALANCHE IMPACT (WITH PILE-UP) ON WALLS AND PYLONS

Perry BARTELT*, Othmar BUSER, Marc CHRISTEN, Andrin CAVIEZEL

WSL Institute for Snow and Avalanche Research SLF, Davos Dorf, Switzerland
e-mail: bartelt@slf.ch

Abstract. *Snow avalanches are a significant natural hazard in many mountainous regions throughout the world. Although long recognized that avalanche impact can easily destroy buildings and other infrastructure, design codes rarely, if at all, consider dynamic magnification factors. The underlying problem is that flowing snow at impact behaves both as a solid and as a fluid. The combination of solid and fluid behaviour makes it difficult to characterize the avalanche impact loading. The solid behaviour of flowing snow leads to pile-up regions of highly compacted snow in front of the structure. This dead-zone often adopts the form of a prismatic wedge with two distinct shear planes. The wedge serves to deflect avalanche snow around the impacted object. Because avalanche snow likewise exhibits fluid behaviour, the deflected snow can easily bypass the structure without stopping. In this paper we model the compaction, pile-up and deflection of avalanche snow around walls, pylons and trees. The work energy theorem is used to model the forces assocated with the compaction process and therefore pile-up phase. We show why the pile-up produces intensive, short duration loadings in the form of a triangular impulse. We quantify the duration time as a function of the pile-up geometry and compactive properties of the flowing snow. This allows us to both quantify the impact duration as well as select the appropriate form of the impulsive loading. If the eigenfrequency of the structure is known, dynamic magnification factors can be calculated for avalanche impact on a wide range of structure geometries, especially ski-lift masts, walls and power transmission towers.*

Keywords: Natural hazards, Snow Avalanche, Impact Loadings, Pile-up, Work-Energy Theorem, Dynamic Magnification Factors, Pylons, Walls.

ISSN:2623-3347
Peer-review under responsibility of the organizing committee of COMPDYN 2019.
doi: 10.7712/120119.7234.20047

1 INTRODUCTION

In mountain environments snow avalanches pose a considerable threat to the built infrastructure [1, 2, 3, 4]. Structural engineers require calculation methods to relate avalanche speed to design loads in order to construct structures that can survive avalanche impact (Fig. 1). At present snow engineering practice applies the generic formula

$$p = \frac{1}{2} C_D \rho_\Phi V_\Phi^2 \tag{1}$$

to caluate the impact *pressure* p as a function of avalanche density ρ_Φ and velocity V_Φ^2 [5]. The pressure factor C_D accounts for avalanches impacting thin (C_D=1) and wide (C_D=2) structures. A more general equation to calculate the impact *force* $F(t)$ on a structure hit by a snow avalanche is,

$$F(t) = F_\Delta(t) + F_\Upsilon(t) + \oint_E f(s,t)\, ds. \tag{2}$$

Figure 1: On March 8, 2017 a snow avalanche destroyed several chalets at the Swiss village of Salvan, Canton Wallis. Impact pressures were higher than 30 kPa. The air-blast from the avalanche blew down several trees behind the buildings. The building on the right was completely destroyed. The picture appeared in the *Walliser Bote* on March 8, 2017.

This formula characterizes the three physical processes that must be considered at impact: (1) the shock loading $F_\Delta(t)$ caused by the solid, entirely plastic "pile-up" of snow mass in front of the structure, (2) the deflection force $F_\Upsilon(t)$ arising from the fluid movement of snow mass around the structure and (3) edge forces $f(s,t)$ which are produced when the deflected snow jams the on-coming avalanche mass at the exterior edges E of the structure. The line integral is given by the fact that jamming forces $f(s,t)$ are defined per unit edge length. The upper limit of the integration is given by the flow height of the avalanche which defines the sum of the exposed edges of the structure. An important distinction between the two approaches is that first approach (Eq. 1) calculates a mean *pressure*, whereas the second approach (Eq. 2) predicts time-dependent *forces* that are assumed to be distributed unequally over the structure at impact.

By far the greatest challenge of developing methods to predict avalanche impact forces is due to the complex solid-fluid behaviour of avalanche snow. The piled-up snow typically forms a solid "deadzone" in the shape of a prismatic wedge (Fig. 2). (Hence there designation with the capital greek symbol Δ.) The wedge consists of highly compacted snow that serves to efficiently deflect the on-coming avalanche snow around the impacted object. That is, at impact both solid and fluid behaviour is evident. The solid material response is complicated further by the irreversible compactibility (or *Stauchen*) of avalanche snow. Bulk avalanche flow densities ρ_Φ range between (say) ρ_Φ = 150 kg/m^3 for a disperse flowing/powder avalanche to (say) ρ_Φ = 450 kg/m^3 for a dense wet snow avalanche [1]. Density measurements of piled-up snow in front of obstacles indicates that final compaction densities are over $\rho_\Delta \geq 500$ kg/m^3 [6]. The dynamic, impulsive loading at impact results from the compaction of the avalanche snow from density ρ_Φ to density ρ_Δ. The time required to compact the snow to build the wedge therefore defines the duration of the impact loading and therefore the rate of energy dissipation and the impulsive (shock) response of the structure.

In this paper we develop a method to calculate how snow piles-up at impact allowing us to estimate the magnitude, form and duration of the impulsive loading $F_\Delta(t)$. This is a necessary prerequisite to determine the shock response (failure) of structures impacted by snow avalanches. We begin by considering forces for pile-up without deflection. This serves to introduce the application of the work-energy theorem to determine forces from the compaction of avalanche snow at impact. We then turn our attention to the more realistic problem of pile-up with deflection. This analysis allows us to determine dynamic magnification factors for simple structures such as cantilever-type constructions such as pylons and masts which are typical for ski-lifts and power transmission lines. We provide several example calculations. The first example considers an avalanche impacting trees, where the eigenfrequencies are low. The second example treats an avalanche impacting a circular ski-lift pylon, a common problem in avalanche mitigation.

2 PILE-UP WITHOUT DEFLECTION: FORCES F_Ξ

For the purpose of explanation we find the force F_Ξ where all avalanche mass piles-up completely at impact in front of the structure (Fig. 3). There is no deflection ($F_\Upsilon = 0$) or jamming ($f(s,t) = 0$). In this case the impact force $F(t) = F_\Xi$.

We consider a dense avalanche Φ with velocity V_Φ, height h_Φ and bulk density ρ_Φ impacting a rigid structure. The structure of width w is positioned at the position x=0; the positive x-direction defining the upstream direction of the pile-up. For simplicity we assume the avalanche strikes the structure with a mean depth-averaged velocity and density; that is, both variables are constant over the flow height defined in the z-direction, but can vary in the streamwise direction and therefore time. We do not consider the impact of the powder dust cloud Π. For now we assume that the height of the structure h is higher than the flow h_Φ i.e. there is no overtopping of the structure. The width of the flow is assumed to be larger than the width of the obstacle.

We describe the pile-up process by considering avalanche mass immediately before and after the pile-up (Fig. 3). All the incoming mass is piled-up. The avalanche is divided into "compacting" avalanche snow, the *knautschzone* (region Ξ, density not yet ρ_Ω, velocity not yet zero,

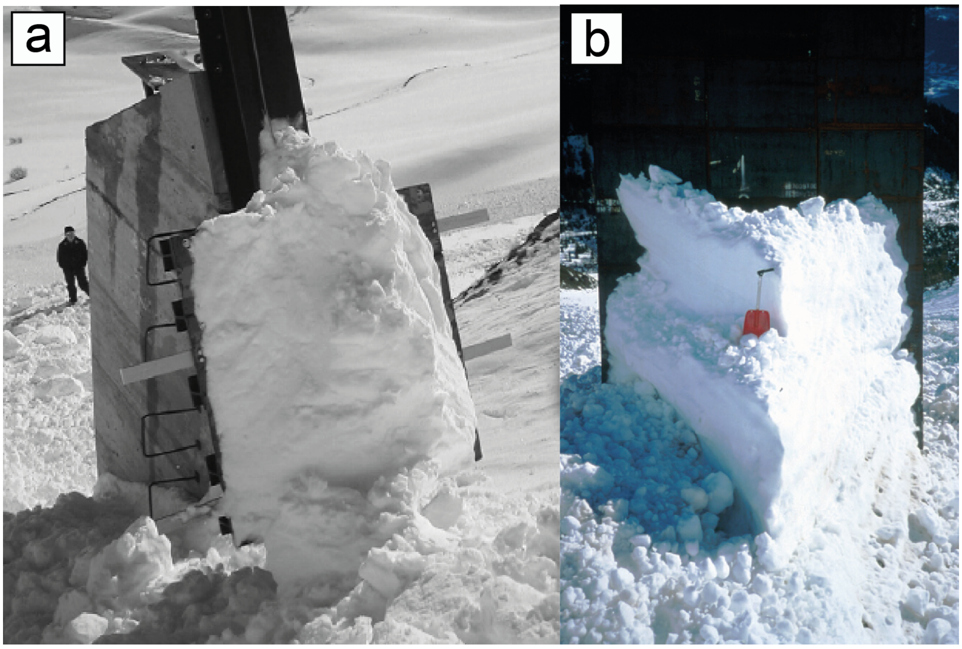

Figure 2: Examples of impact wedges. a) Pile-up at the measurement pylon at the French Col du Lautaret test site reported by [6]. Note the dihedral shape of a triangular prism. The width of the impact plane is 1 m. The reported compaction density was 540 kg/m^3; wedge angles ω_1=40° and ω_2=50°, impact pressures of 30 kPa, see [6] for details. b) Pile-up at the measurement wall at the Swiss Vallée de la Sionne test site [7]. The wall is 7m high and 3.5 m in width. The impact wall was designed to resist 500 kPa pressures. The depositions are from an wet snow avalanche recorded on December 12, 1998 with maximum recorded forces of 61 kN. Measured densities are 500 kg/m^3 at the wedge apex and 450 kg/m^3 at the wall. Photograph: M. Kern, SLF

time t) and "compacted" avalanche snow (region Ω, density ρ_Ω, no velocity, time $t+\Delta t$). Measurements of compacted snow density are rare. Thibert [6] measured a pile-up density ρ_Ω of 540 kg/m^3 in front of the instrumented pylon at the French Col du Lautaret test site.

The avalanche mass arriving at the obstacle M_Ξ and stopping within the time interval Δt is

$$M_\Xi = \rho_\Phi h_\Phi w \left[V_\Phi \Delta t \right]. \tag{3}$$

The corresponding change of kinetic energy ΔK_Ξ of the avalanche is therefore

$$\Delta K_\Xi = \frac{1}{2} M_\Xi(t) V_\Phi^2 = \frac{1}{2} \rho_\Phi h_\Phi w \left[V_\Phi^3 \Delta t \right]. \tag{4}$$

The length of the compacted, pile-up zone is denoted S_Ω, the height h_Ω. The pile-up height might be larger than or equal to the incoming avalanche height $h_\Omega \geq h_\Phi$. Because we do not have overtopping, we assume it remains smaller than the height of the obstacle $h_\Omega < h$. The length of the pile-up zone is growing at the rate $\dot{S}_\Omega$; it is given by conservation of mass,

$$\dot{S}_\Omega = \frac{\rho_\Phi(t) h_\Phi(t)}{\rho_\Omega h_\Omega} V_\Phi(t). \tag{5}$$

During the pile-up, the region Ξ of length $V_\Phi(t)\Delta t$ in the x-direction compacts, increasing the length of the compaction zone Ω (Fig. 3). The difference in the locations of the center-of-mass of the compacting zone Ξ and the piled-up mass Ω defines the braking distance $d_{\Xi\to\Omega}$ over which the incoming mass must stop,

$$d_{\Xi\to\Omega} = \frac{1}{2} \left[V_\Phi \Delta t - \dot{S}_\Omega \Delta t \right]. \tag{6}$$

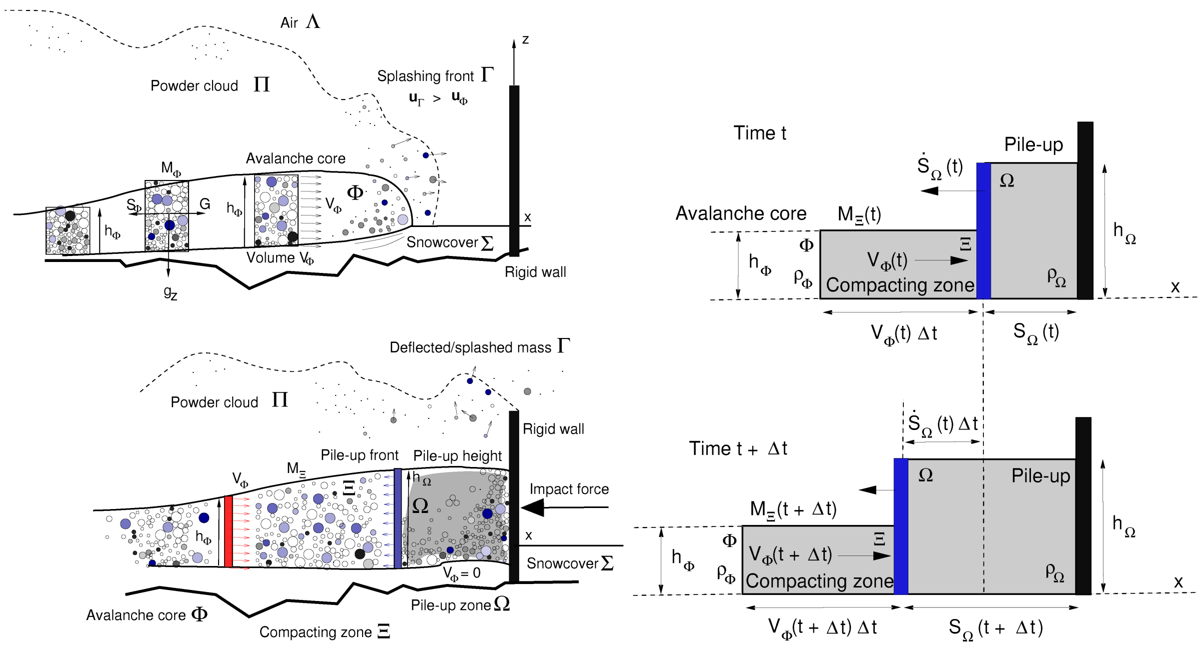

Figure 3: Avalanche impact with no deflection. The upstream zone is divided into three regions: the dense flowing avalanche Φ, the compacting region Ξ and the pile-up or accumulation zone Ω. The avalanche arrives at time t travelling with the velocity V_Φ, bulk density ρ_Φ and flow height h_Φ. Within the time interval Δt the *knautschzone* Ξ develops in front of the structure with length $V_\Phi \Delta t$. A pile-up zone Ω with length S_Ω forms. The pile-up zone is increasing at the speed $\dot{S}_\Omega$.

The mean force on the obstacle F_Ξ is found by equating the work-done by the braking and the change of kinetic avalanche energy in the compaction zone ΔK_Ξ,

$$F_\Xi d_{\Xi\to\Omega} = [p_\Xi h_\Omega w]\, d_{\Xi\to\Omega} = \Delta K_\Xi \tag{7}$$

or,

$$F_\Xi = \rho_\Phi h_\Phi w \frac{V_\Phi}{\left[V_\Phi - \dot{S}_\Omega\right]} V_\Phi^2 \tag{8}$$

The impact pressure p_Ξ is found assuming the force is applied uniformly over the impact area $h_\Omega w$. Therefore,

$$p_\Xi = \rho_\Phi \frac{h_\Phi}{h_\Omega} \frac{V_\Phi}{\left[V_\Phi - \dot{S}_\Omega\right]} V_\Phi^2 \tag{9}$$

and with the subsitution of the equation for mass conservation

$$p_\Xi = \rho_\Phi \frac{h_\Phi}{h_\Omega} \left[1 - \frac{\rho_\Phi h_\Phi}{\rho_\Omega h_\Omega}\right]^{-1} V_\Phi^2. \tag{10}$$

It is therefore possible to define an pressure factor C_D for the pile-up without deflection regime,

$$C_D^\Xi = 2\frac{h_\Phi}{h_\Omega} \left[1 - \frac{\rho_\Phi h_\Phi}{\rho_\Omega h_\Omega}\right]^{-1}. \tag{11}$$

Note that the pressure factor becomes infinite when $\rho_\Phi h_\Phi = \rho_\Omega h_\Omega$. These values of equivalent C_D are in agreement with measured values for all $\rho_\Omega > \rho_\Phi$, see Fig. 4b, and compare to

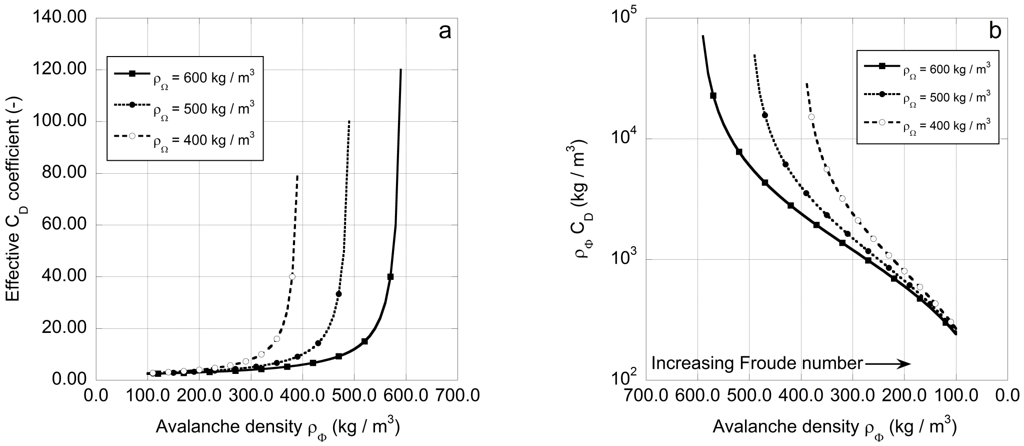

Figure 4: a) Effective C_D^Ξ coefficient (Eq. 11) for different incoming avalanche densities ρ_Φ and three compaction densities ρ_Ω. The flow height and pile-up heights are equal $h_\Phi = h_\Omega$. Large effective C_D coefficients result when $\rho_\Phi \approx \rho_\Omega$. In this case compacting (braking) distances are short and impact pressures are large. b) The calculated $\rho_\Phi C_D$ are in agreement with values derived from full scale measurements, e.g. [8]. For the sake of comparison to measured values we plot the calculated $\rho_\Phi C_D$ values with decreasing density to mimic increasing Froude numbers (higher Froude numbers correspond to lower flow densities). This produces the effect that effective pressure factors C_D are higher for lower flow velocities.

[8]. This result suggests that impact pressures of slow moving avalanches can be large if the density of the incoming avalanche is near the compaction density. Substitution of Eq. 1 into the work-energy theorem (Eq. 8) leads to

$$C_D^\Xi = \frac{V_\Phi \Delta t}{d_{\Xi\rightarrow\Omega}}. \tag{12}$$

The pressure factor is therefore the length of the *knautschzone* Ξ relative to the braking distance $d_{\Xi\rightarrow\Omega}$.

3 PILE-UP WITH DEFLECTION: FORCES F_Δ

We again consider a dense avalanche Φ impacting a rigid structure with velocity V_Φ, height h_Φ and bulk density ρ_Φ. This time, however, a prismatic wedge forms at the face of the structure and avalanche snow is deflected (Fig. 5). We assume symmetry (a head-on interaction with the structure). The structure of half width w_0 is positioned at x=0; the positive x direction defining the incoming avalanche direction; the y direction is defined along the width of the obstacle. The total width of the obstacle is therefore 2 w_0. We make the same avalanche flow assumptions as for the previous case.

In the time interval Δt the incoming mass of the avalanche core M_Φ is partitioned into two parts. The mass that is deflected M_Υ and the mass that is piled-up in a triangular wedge M_Δ

$$M_\Phi = \underbrace{\rho_\Phi h_\Phi w V_\Phi \Delta t}_{\textit{Incoming mass}} = \underbrace{M_\Upsilon}_{\textit{Deflected mass}} + \underbrace{M_\Delta}_{\textit{Wedge mass}}. \tag{13}$$

The mass piled-up on the wedge per unit width (y-direction) m_Δ is

$$m_\Delta(y) = \left(1 - \frac{y}{w}\right) \rho_\Delta h_\Delta \dot{S}_\Delta \Delta t. \tag{14}$$

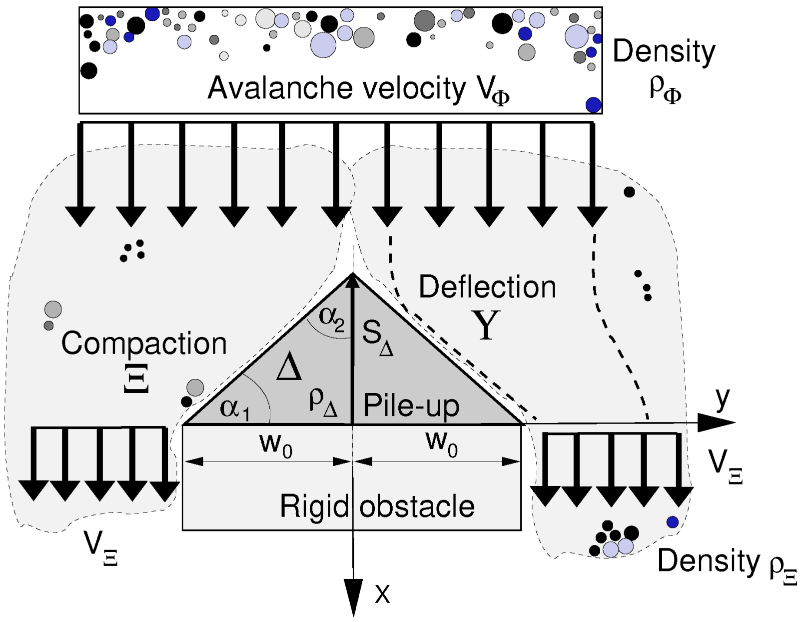

Figure 5: Definition of wedge-shaped pile-up with deflection plus compaction in front of the obstacle. The avalanche approaches the obstacle in the positive x-direction with velocity V_Φ. The bulk density of the flow is ρ_Φ. A pile-up wedge Δ is formed. The density of the piled-up snow is ρ_Δ. The length of the wedge in the flow (negative) x-direction is S_Δ. The speed the length of the triangular wedge grows is $\dot{S}_\Delta$. The wedge geometry is defined by the angle α_1 with α_2 = 90° - α_1.

where S_Δ is the length of the wedge in the x-direction at the location x=0, see Fig. 5. The speed the wedge is growing is therefore $\dot{S}_\Delta$. The total mass of the snow pile up is found by integration

$$M_\Delta = \int_0^w m_\Delta(y)dy = \frac{1}{2}\rho_\Delta h_\Delta w \dot{S}_\Delta \Delta t. \tag{15}$$

The loss of kinetic energy $k_\Delta(y)$ per unit length in the y-direction is

$$k_\Delta(y) = \frac{1}{2}m_\Delta(y)V_\Phi^2 = \frac{1}{2}\left(1 - \frac{y}{w}\right)\rho_\Delta h_\Delta \dot{S}_\Delta V_\Phi^2. \tag{16}$$

The kinetic energy is lost over the "braking" distance

$$d_{\Phi\to\Delta}(y) = \frac{1}{2}\left[V_\Phi \Delta t - \left(1 - \frac{y}{w}\right)\dot{S}_\Delta \Delta t\right]. \tag{17}$$

From the work-energy theorem, the force per unit length f_Δ is applied

$$f_\Delta d_{\Phi\to\Delta} = k_\Delta. \tag{18}$$

Therefore,

$$f_\Delta = \frac{k_\Delta}{d_{\Phi\to\Delta}} = \frac{\left[\left(1 - \frac{y}{w}\right)\dot{S}_\Delta\right]}{\left[V_\Phi - \left(1 - \frac{y}{w}\right)\dot{S}_\Delta\right]}\rho_\Delta h_\Delta V_\Phi^2 \tag{19}$$

This value can be integrated over width of the triangle w (y-direction) to find the mean pile-up force F_Δ on the obstacle

$$F_\Delta = \int_0^w f_\Delta(y)dy = \left[\frac{V_\Phi}{\dot{S}_\Delta}\ln\left(\frac{V_\Phi}{V_\Phi - \dot{S}_\Delta}\right) - 1\right]\rho_\Delta h_\Delta w V_\Phi^2. \tag{20}$$

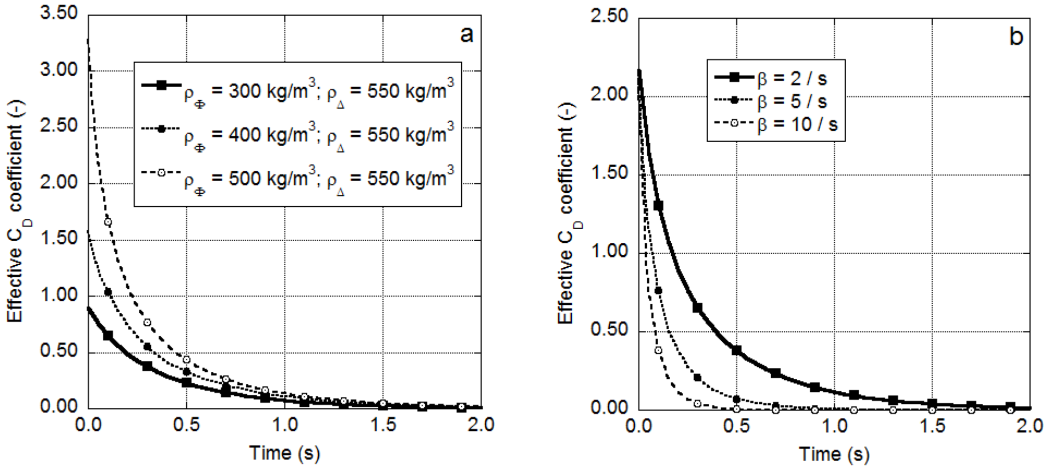

Figure 6: a) Effective C_D^Δ coefficient (Eq. 22) for different incoming avalanche densities ρ_Φ and three wedge pile-up densities ρ_Δ. The flow height and pile-up heights are equal $h_\Phi = h_\Omega$. Large effective C_D^Δ coefficients result when $\rho_\Phi \approx \rho_\Delta$. b) Effective C_D^Δ coefficient (Eq. 22) for different β values. Note that the pile-up times vary between 0.25s and 1.0s.

The pile-up pressure acting on the rigid obstacle is

$$p_\Delta = \frac{F_\Delta}{w h_\Delta} = \left[\frac{V_\Phi}{\dot{S}_\Delta} \ln \left(\frac{V_\Phi}{V_\Phi - \dot{S}_\Delta} \right) - 1 \right] \rho_\Delta V_\Phi^2. \tag{21}$$

The pressure retains a V_Φ^2 dependency with the pre-multiplier serving as the pressure factor C_Δ,

$$C_D^\Delta = 2 \left[\frac{V_\Phi}{\dot{S}_\Delta} \ln \left(\frac{V_\Phi}{V_\Phi - \dot{S}_\Delta} \right) - 1 \right] \tag{22}$$

At present the model contains no constitutive parameters. The quantity $\dot{S}_\Delta$ controls the duration of the wedge formation and therefore the duration of the pile-up loading. We consider the growth of the wedge to be given by the relationship

$$\dot{S}_\Delta = \frac{\rho_\Phi}{\rho_\Delta} V_\Phi \exp\left(-\beta t\right). \tag{23}$$

The coefficient β (dimension 1/s) therefore describes the partitioning of the incoming mass into the deflected and piled-up mass. At a certain time, when the wedge is sharp enough, the growth of the wedge stops. Clearly other constitutive formulations can be postulated. The pressure factor C_D^Δ is a function of time, see Fig. 6.

4 RESULTS: DYNAMIC MAGNIFICATION FACTORS

The results of the preceeding section (Fig. 6) demonstrate that the impact pressure for pile-up p_Δ is well represented by a triangular impulse of the form

$$p_\Delta \approx p_\Delta(0) \left[1 - t/t_1\right] \tag{24}$$

where t_1 defines the duration time of the impulse. The dynamic magnification factor D for triangular impulse loadings are treated in standard structural dynamics texts, see [9]. Table

1 presents D values for various impulse length t_1/T ratios (T is the period of vibration of the impacted structure). Periods of vibration for steel pylons and trees can be found using Rayleigh's method treating the structure as a partially loaded cantilever beam [10]. At the ground the structures are fixed allowing no translational deformation or bending rotations. The flow height of the avalanche defines the region on the cantilever which is loaded at impact.

t_1/T	0.20	0.40	0.50	0.75	1.00	1.50	2.00
D	0.60	1.05	1.19	1.38	1.53	1.68	1.76

Table 1: Dynamic magnification factors for triangular impulse loadings, from [9].

The first practical result of our analysis is that pylon-type structures with eigenfrequencies of greater than 5Hz (approximately) should consider dynamic magnification factors in design and back analysis. Interestingly, mature spruce trees, typical for most mountain environments have eigenfrequencies of ω = 1Hz (and lower) [10, 11] and therefore long periods of vibration $T \approx 6$ s. From the results above we find pile-up loading intervals $0.25 \leq t_1 \leq 1.0$ s. The calculated impulse length ratios are between $0.04 \leq t_1/T \leq 0.17$. The dynamic magnification factors for trees are less than 1 meaning that $0.1 \leq D \leq 0.6$ (Table 1). This result indicates that trees are able to withstand short duration avalanche pile-up loadings, but are remain susceptible to longer duration air-blasts. This result would explain the extensive forest damage caused by powder avalanches and the fact that many trees can withstand the impact of fast moving avalanche cores, see Fig. 1.

For the next example problem we consider a circular ski-lift pylon made of steel with a height of H= 15m and diameter of d = 1m. The thickness of the steel section is 3cm. The pylon is struck by an avalanche with flow height h_Φ = 3m. For this loading, the calculated eigenfrequency of the pylon is approximately ω = 80 Hz, the period of vibration $T \approx$ 0.08s. Calculated impulse length ratios are $t_1/T > 3$, indicating large dynamic magnification factors D = 1.76 (Table 1). Unlike trees, rigid steel structures appear to be more vulnerable to impulsive pile-up loadings.

Finally we consider the impact forces on wall depicted in Fig. 2b [7]. This wall has a total width of 3.5m. Measured maximum reaction forces on the right, center and left supports are 29kN, 61kN and 49kN respectively for a wet snow avalanche impacting the wall with a 4m flow height and velocity of 4.6m/s. The length of the pile-up wedge was found to be 2m. This pile-up height can be reproduced using a β=1.5/s. The calculated reaction forces from Eq. 20, assuming a direct hit, are 38kN, 63kN and 38kN.

5 CONCLUSIONS

In this paper we have applied the work-energy theorem to calculate the magnitude, form and duration of the impulse loading that results when mass is piled-up in the form of prismatic wedge. We consider two cases – pile-up without deflection (force F_Ξ) and pile-up with deflection (force F_Δ). The model assumes a single constitutive parameter (β) that defines the loading interval which can be compared to the vibration period of the impacted structure. Dynamic magnification factors can therefore be calculated and used in structural design. An interesting and unexpected result of our analysis is that trees appear to have low magnification factors $D \leq 0.5$, in comparison to rigid steel structures $D \geq 1.5$. This result would help explain the usefulness of forests in avalanche defense and the danger caused by avalanches to the built environment.

REFERENCES

[1] Bozhinskiy, A. N., and Losev, K. S. *The fundamentals of avalanche science*, Mitt. Eidgenöss. Inst. Schnee- Lawinenforsch., Davos. 280 p., 1998.

[2] Bertrand, D., Naaim, M., and Brun, M.: Physical vulnerability of reinforced concrete buildings impacted by snow avalanches, *Nat. Hazards Earth Syst. Sci.*, 10, 1531-1545, https://doi.org/10.5194/nhess-10-1531-2010, 2010.

[3] De Biagi, V., B. Chiaia, B. Frigo, Barbara, Impact of snow avalanche on buildings: Forces estimation from structural back-analyses, *Engineering Structures*, 92, 15-28, 2015.

[4] Ousset, I., D. Bertrand, M. Brun, E. Thibert, A. Limam, M. Naaim, Static and dynamic FE analysis of an RC protective structure dedicated to snow avalanche mitigation, *Cold Regions Science and Technology*, 112, 95-111, 2015.

[5] Salm, B. A. Burkard and H. Gubler, Berechnung von Fliesslawinen: Eine Anleitung für Praktiker mit Beispielen, Mitt. Eidgenöss. Inst. Schnee- Lawinenforsch., Davos. 30 p., 1990.

[6] Thibert, E., D. Baroudi, A. Limam, P. Berthet-Rambaud, Avalanche impact pressure on an instrumented structure, *Cold Regions Science and Technology*, 54(3), 206-215, 2008.

[7] Gruber U. and 7 others, Lawinendynamik-Versuchsgelände Vallee de la Sionne, Arbaz, Wallis Schulssbericht Winter 1998/1999, Interner Bericht Eidgenöss. Inst. Schnee- Lawinenforsch., Davos. 120 p., 2002.

[8] Sovilla, B., M. Schaer, M. Kern, P. Bartelt, Impact pressures and flow regimes in dense snow avalanches observed at the Vallee de la Sionne test site, *Journal of Geophysical Research-Earth Surface*, 113(F1),DOI: 10.1029/2006JF000688, 2008.

[9] Clough R.W and J. Penzien, *Dynamics of Structures*, McGraw-Hill Inc, New York, 634p, 1975.

[10] Bartelt, P., P. Bebi, T. Feistl, O. Buser, A. Caviezel, Dynamic magnification factors for tree blow-down by powder snow avalanche air blasts, *Natural Hazards and Earth System Sciences*, 18(3), 759-764, 2018a.

[11] Feistl, T., P. Bebi, M. Christen, S. Margreth, L. Diefenbach, P. Bartelt, Forest damage and snow avalanche flow regime, *Natural Hazards and Earth System Sciences*, 15(6), 1275-1288, DOI 10.5194/nhess-15-1275-2015.